PINCHED CAVITATION JETS AND FUSION EVENTS

Roger S. Stringham
First Gate Energies
PO Box 1230, Kilauea, HI, 96754. USA - email <firstgate@earthlink.net>

ABSTRACT

The collapse of a transient cavitation bubble in deuteriumoxide produces a high density plasma jet containing 10^9 deuterons. The inertial compression of a jet via an electron induced magnetic field pinch effect on its plasma contents produces high to even higher deuteron densities in the order of 10^{25} gm/cc before implanting into a foil target. This model is parallel to the systems found in the hot plasmas of inertial systems. During the initial period of implantation of a few picoseconds, the high density deuterons in the target lattice experience reduced coulomb repulsion due to the high density charge screening. In this environment it is possible that some DD fusion events occur as evidenced by photos of the metal target foils and by the evidence of helium four and tritium production.   Making some basic assumptions the smallest diameter and highest population of vent sites in the target foils are produced by events in the order of 20 Mev.   When experiments were monitored there was no long range radiation detected.

1. INTRODUCTION

This paper draws from many years of data collection from experiments that produce transient cavitation bubbles, TCBs, collapsing on various targets. Reducing the thinking to cause and effect we have the TCB as the initiator and the nuclear events as the result.   Between these two points we try to find a reasonable path.   To place this work in its proper perspective one should examine some hot fusion experimental procedures [1], magnetic confinement fusion, MCF [7], inertial confinement fusion, ICF [2], and muon fusion, MF [3,4]. The transient high density systems produced by the cavitation jet plasma draw from the physics of the above processes.   The high densities produced by the laser compression of the ICF systems, the magnetic pinch analysis of the MCF systems, and the reduced radius (high density) of DDμ in the MF systems all contribute to understanding the feasibility of cavitation fusion [1-7]. Much of the data can be explained using a model consisting of a very fast moving eight step sequence of events including bubble collapse, target implantation, target lattice high density deuteron transient traps, and high density fusion events.

An acoustic field generation of TCBs in D_2O, ranging from 10 to 50 cc in a reactor device is mechanically driven at its resonant frequency incorporating one or two piezos per reactor. The TCB requires a higher energy input (larger acoustic pressure differential) in the sinusoidal pressure field than in the stable cavitation bubble [8].   The TCB acoustic input must be compatible with the liquid temperature and the external pressure creating an environment for the production of TCBs and multi-bubble sonoluminescence, MBSL. The cycling acoustic pressure wave at the reactor resonant frequency and amplitude drives a selection of proto bubbles of uniform size from its low pressure node through the node towards its high pressure antinode at a magnitude of several atmospheres above the vapor pressure of the D_2O liquid.   The intensity of MBSL and SBSL (multi bubble and single bubble sonoluminescence) depends on the frequency, acoustic pressure, external pressure, and temperature of the liquid [9].   The relationship between the intensity of the acoustic pressure field, the temperature (vapor pressure) and the external pressure define the zone of MBSL occurrence.

2. EXPERIMENTAL

Experiments completed at LANL produced a substantial amount of ^4He, which was measured in a DOE laboratory.   The following is a description of experiments with the collection of the gas samples for the MS analysis.   The apparatus was a vacuum tight double chamber with a sonication chamber consisting of a sonicator, H_2O and N_2 and a reactor chamber consisting of a target foil, D_2O, and Ar separated by a 500μ stainless steel disk.   A Pd target foil supplied by LANL, 254μ thick and 50x50 mm in area was placed into the reactor and 110 ml of D_2O was added and pressurized with 50 PSIG of Ar gas, ^4He free with less than 0.5ppm ^4He, which was added over the degassed reactor D_2O. The flow rate for the D_2O through the reactor was 180 ml/min and H_2O flowed through the sonicator at a rate of 600 ml/min.   The nitrogen pressure over the H_2O in the sonicator was 72 PSIG across the reactor volume, between the stainless steel disks.   The data collection from the experiment included 13 thermocouples which were read at one minute intervals.   The data, for this

flow through cavitation reactor experiment was collected over a 19 hour period at steady-state conditions and was.compared to cooling curve data.[10]

3. EXPOSED FOIL ANALYSIS

The low energy high density transient deuteron plasma (LEHDP) implanted into the lattice created an environment for fusion events. These events were graphically revealed in FE SEM (field emission scanning electron microscope) photos of the exposed target foils. The eight point path, discussed below, starts from the creation of the TCB that culminates in a unique nuclear process and ends with the creation of the target foil vent site. When the environment for the fusion events is present, the exposed target foil preserves in its frozen metal matrix a vent site population distribution ready for a leisurely FE SEM photo examination.

The lattice of the target foil is the locale for the transient deuteron traps which are fed by the TCB pinched jet plasmas that implant deuterons (a micro deuteron accelerator). It can be demonstrated via the DD rate equations that the close proximity of high density deuterons, the average distance from one another, for a picosecond may reduce the coulomb barrier to a level approaching that of the separation that exists in a deuteron deuteron muon system, (MF) [3,4]. The strong repulsion that comes into play is altered by the transient Bose-Einstein, BE, like environment producing deuteron coherence. Two deuterons in this population having close proximity for a given time will fuse, forming ^{4}He and heat but no long range radiation.

The heat pulse, generated by nuclear events deep in the target foil, travels to and erupts from the surface as ejected vaporous metal with the resulting formation of vents in the target foil. These vent sites are found covering the foil's exposed surface in FE SEM photos. One sq. μm of the target foil surface indicates the random population density of the smaller vent site sizes and shows a numerical maximum of sites with an ejecta energy of about 20 Mev [11]. This value is close to the energy of one DD fusion event. Our report in ICCF8 shows the distribution of the vent site population and the expected population of jet plasma implants generated from the TCB. The associated energy expected from an implant does not fit that of the ejecta site population found in the foil target. The ejecta which does not contain the implant energy but the heat of the DD fusion events. The vent sites do not correlate with the implant process. The jet plasma implants are similar in energy originating from proto bubbles of a similar size. Therefore, an implant vent size should lie in the range of 1500 nm a diameter, twenty times that of the vent site. An implant population distribution was not observed on the Pd target foil [11].

4. A PATH TO SONO FUSION

The path that is described here as an eight step process which fits the bulk of the data that has been gathered over the years. The process starts in the D_2O with proto bubbles of radius, R_i, that are residual from the previous acoustic cycle. The acoustic wave progresses through the liquid in its the pressure phase. The bubble grows isothermally, gaining mass, which partially fills the vacuum created by the expanding bubble. As the momentum of D_2O, the liquid surrounding the bubble, expands away from the bubble center, the D_2O vapors and aerosols from the bubble interface migrate increasing the bubble mass. This isothermal mass growth continues as the acoustic pressure wave crosses the node into its high pressure phase. The bubble growth slows and then stops at its maximum radius, R_0, and closes the isothermal growth process. End of step - 1

What follows is a rapid collapse process, adiabatic in nature, as the acoustic pressure continues to increase [9]. Although the bubble has accumulated a small amount of D_2O vapor, it is still essentially a vacuum, depending on acoustic input, frequency, temperature, and pressure. The increasing pressure reverses the direction of momentum and initiates the bubble collapse with the surrounding D_2O mass accelerating the bubble contents and its interface towards the bubble center. This rapid event is less than a μ second, at 40 KHz, where the driving force originates from an attempt to equilibrate the differential pressure between the external pressure over the D_2O and the internal pressure of the partial vacuum of the bubble contents. In the adiabatic collapse process the bubble contents are heated by compression to the point of dissociation producing ions and free electrons, to form a low energy high density plasma, LEHDP. This LEHDP is responsible for the production of sonoluminescence photons and plasma containing jets. End of step - 2.

The LEHDP plasma jet is produced at the end of the adiabatic bubble collapse process. The jet contents consist of electrons and ions which are pinched via the magnetic field produced by the high velocity of plasma electrons. The pinch of the LEHDP jet, during the transient time period, from the collapsed TCB to the target surface, compresses the jet contents. The jet is about a micron in length and 0.1 or less in radius and is compressed as it extends. At the time of implantation the LEHDP jet is at a maximum density. The D+ and e- plasma density is compressed by the z pinch effect from the high velocity sheath electrons. These electrons, initially associated with the bubble interface, will form a thin containment sheath around the plasma jet. In the jet the density of the particles is increasing and the surface electrons move in a spiral with respect to the slower

more massive deuterons. It is the nature of the plasma, unlike particle beams where the forces between particles have little influence on each other, to flow as a cohesive body as long as the particle distance does not exceed the Debye length. The bubble contents are accelerated and implanted into nearby target surfaces. End of step - 3

The contents of the jet plasma are mostly deuterons and electrons in one form or another and are energetically coherent. [11]. The high velocity of the LEHDP electrons produces a z pinch further increasing the jet density. There is a strong transient coulomb field produced, at the point of lattice implantation, between the implanted electrons and deuterons. The implantation of LEHDP electrons deep into the lattice are followed by deuterons to a lesser depth. End of step - 4

The pinched jet plasma implants into the target lattice with interactions that are not fully understood. Fusion events will occur under the right conditions. The LEHDP jet implants high density deuterons into the lattice of the target foil. Diffusion and the dispersing coulomb field limit the deuteron fusion contact time τ. Reducing the repulsion between deuterons through the creation of coherent condensed phase ion traps, liquid or solid phase, in the target foil is similar to those presented in a paper by Young Kim and Alexander Zubarev, ICCF8; Lerici, Italy, May 21-26, 2000 [12]. However, we consider these transient ion traps of high density and temperature having some of the properties of a BE condensate, as speculative End of step - 5.

The environment, which exists for a picosecond, allows for the production of DD fusion events with a LEHDP jet density of 10^{25} D+/cc, a radius of 0.1 µm, a length of 1 µm, and a population of 10^9 deuterons. (These values are all approximate - average.) The τ for these high density deuteron fusion systems is short (about a picosecond) so to compensate one looks for densities that approach those of MF in the deuteron traps (in the range of 10^{25} D+/cc or more). The DD fusion occurs within a few picoseconds in spherical coherent ion traps in
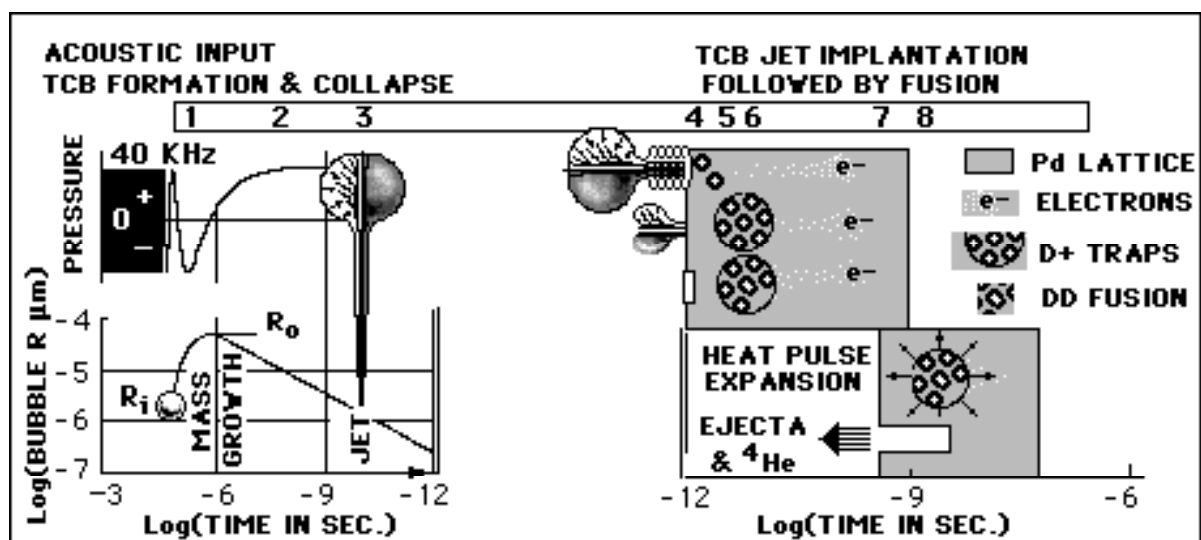

Fig. Eight step path of the TCB in deuteriumoxide and the jet implantation into the reactor target producing fusion events.

the target lattice with a radius of about 600 D+ ions at the implant density or about 60 nm. These densly populated D+ traps have some of the characteristics of the BE condensate. The implanted deuterons, collected in the ion traps are detained momentarily, cause a transient charge separation in the implant lattice. The coulomb barrier between lattice trapped D+ is altered through the cancellation of the repulsive charge between the population of interior D+ in the trap. The deuteron trap rapidly loses its collection of D+ through diffusion and combination (2D$\rightarrow$ D$_2$). Fusion occurs without long range radiation [12]. End of step - 6.

There is a period of a few picoseconds in the lattice traps where one or more heat producing fusion events can occur and in the process destroy the transient D+ trap collection. There is an intense heat pulse generated from fusion events located in the lattice ion trap. There may be one or many fusion events that occur from one LEHDP jet implantation. This heat radiates out from its source in the lattice as a gaseous vapor to the surface boundary of the target foil. It bursts from the target surface as a metallic vapor ejecta leaving a footprint that can be photographed [11]. End of step - 7.

The lattice vent sites from these events can be observed in FE SEM photos of metal targets [11]. If conditions are present, high deuteron densities in the deuteron traps and τ in the picosecond range, fusion events occur and are observed as vent sites. These vent sites are the result of the escape of the vaporous metal and gases from the foil target and have a population correlation to a minimum energy near 20 Mev. End of step - 8

The implanted deuterons exist in the target lattice traps as coherent ions in a state much like the BE condensate but at high densities, at temperatures above ambient, and in a very short time frame. There is a window of opportunity for DD fusion events to occur before diffusion and coulomb effects break the coherence of the trapped self-screening deuterons in the target foils traps [2,12]. The fusion events result in the generation of large heat pulses producing the vents in the target lattice and the nuclear products such as ^{4}He and T [11,13]. These vents are easily detected in the cavitation exposed metal target foils via FE SEM photographs. When the LEHDP jet is compared to hot plasma DD fusion, which operated at the low density of 10^{15} D+/cc, an extrapolation to the very high densities of the LEHDP jet created an environment similar to MF. These fusion events produce nuclear products and heat. The D+ was converted to T, p, ^{4}He, ^{3}He, and heat. See figure.

5. THE PINCH EFFECT

The TCB produced jet plasma is squeezed by a magnetic pinch to even higher densities. Assuming a HDLEP jet configuration of cylindrical dimensions in step - 3 of A PATH TO SONO FUSION a rough estimate can be made of the z pinch. The current in amps produced in a jet is $I = dQ/dt = QvA$ where Q is the coulomb charge, v is the velocity of the sheath electrons in meters per second and A is the area of the jet in m^2. Q relates to the number of electrons that pass through one square meter, A, at a velocity in meters/sec. The velocity is that which is produced in the dissociation of D_2 and D_2O (about $1.5x10^5$ Kcal/Mole) and relates to an electron velocity of about $3x10^6$ m/s. The number of deuterons in a jet plasma, for example, is $3x10^8$ with several times that number of electrons. The cross-section area of the jet is $3x10^{-14}$ m^2. These numbers show a jet current of 130 amps [1]. The magnetic z-pinch confinement by the amps generated in the jet is $B = \mu I/(2\pi r)$ where $\mu = 4\pi x10^{-7}$ and .B = 260 Tesla.

TCB photos and theories of the bubble jet have been featured in several papers [16-19]. The magnetic pinch pressure and the escape pressure reveal the jet's likelihood for its progressively increasing density. The pinch pressure $= 1/8\pi(I/(5r))^2$ and the escape pressure $= nkT$ oppose each other, where I is the current generated by the jet and r is the jet radius. The Boltzmann constant k and the density of electrons, n (e-/cc). When the pinch force is greater than the outward force, the jet is contained and further compressed to higher densities. The change in the density of ionized D_2O in the jet plasma holding parameters T, v, and r constant shows that n affects the jet's confinement. The escape force varies as n, but the pinch force varies as n^2. For greater values of n the resulting compression force on the jet contents is $(1/8\pi(I/(5r))^2 - nkT)$ The n^2 term is in I^2 of the pinch. The transient nature of the increasing pinch effect is a few picoseconds.

The escape of the unidirectional jet particles is related to the temperature of the plasma. If the escape pressure in the HDLEP jet is less than the magnetic pinch pressure, the resulting pressure difference is that of a jet under the influence of the pinch effect. The stability of the jet that appears so often in photographs of the bubble collapse process is accounted for by the magnetic pinch being dominant over the escape pressure [1].

6. RATE OF FUSION IN TARGET FOIL

A DD reaction rate can be estimated through the examination of the FE SEM photos of the target foil surface ejecta site count. Jet plasma and ion beam implantation are systems of particles that differ in their density (plasma particle separation is less than the Debye radius). The jet plasma is cohesive and behaves as a fluid and not as a stream of particles. As photographs show, a plasma (LEHDP) will traverse 10μ, more or less, into the lattice to the birthplace of the vent sites. On the other hand the range of a low energy ion beam of deuterons at a density of 10^{14} D+/cc traverse only to the surface of the target foil one atomic layer deep [20-22]. The jet LEHDP first implants the more mobile electrons into the target foil followed closely by the deuterons. The other ions, Ar^+ and O^+, may be screened from deep lattice penetration by their comparative large size and low velocities. The fusion events produced, by the implantation of deuterons into a metal foil lattice, the products T, p, ^{4}He and ^{3}He, and heat[13,14].

A LEHDP jet generated from the collapsing cavitation bubble in D_2O becomes a micro accelerator that implants deuterons into a target foil. At our target there are perhaps 5000 jets formed in each acoustic cycle and for a 40 KHz acoustic input there are perhaps 200 million jets formed per second. The rate for one jet implantation into a target foil has a DD fusion rate considering a one cc volume during a one second interval of $R_{DD}=.5n^2v\sigma$. This rate is modified by multiplying by a constant, K, so the rate refers to the deuterons

implanted by the jet volume during the fusion contact time, τ. $KR_{DD} = K\ 0.5(n)^2\sigma v = R_{DD}/J$.   The DD fusion rate per implanted jet depends on the density of the deuterons/cc, n, and the implanted deuterons in lattice traps in the target foil.   The fusion cross section, $\sigma = 10^{-26}cm^2$, is based on that of DDμ fusion which is approached by the implantation process [4].   The rate is based on the jet velocity, v, of deuterons at 10^6 cm/sec, a jet volume, V, of 3×10^{-18} cc and a fusion contact time, τ, of 10^{-12} seconds.   The K for the implanted jet fusion rate is $\tau V = 3\times10^{-30}$.   The implanted deuterons exist in the target lattice traps as coherent ions in a transient state perhaps analogous to a BE condensate for just a few picoseconds.   We assume that the density of deuterons in the jet is transferred through the implantation process to the target lattice where the deuteron fusion occurs.   K, which is the proportionality constant for R_{DD}/J, gives a value for the number of fusion events per jet implantation.

7. DOE ANALYSIS of ^{4}He and He^3 (T)

The collected gases were analyzed using a simple gas handling system to remove the gas from over the D_2O in the reactor into a sampling volume.   A blank run (a non helium producing run 4 - 1) via gas analysis of the argon in the reactor gave an upper limit in the argon supplied by LANL for ^{4}He.   Sample cylinders were initially evacuated, then pressurized with the gases collected from over the reactor (mostly argon gas with small amounts of product gases) admitted by expansion from the reactor.   The sample cylinders were stainless steel, of all welded construction, having a 50cc capacity and a 6 mm inlet valve.   The D_2O from Aldridge and the argon from Air Products was provided by LANL.   These labeled gas filled sample cylinders were delivered to the DOE laboratory facilities at Rockwell Int. at Canoga Park, CA where Brian Oliver analyzed them for ^{3}He and ^{4}He.   The methodology was to remove a small amount (1 to 2%) of gas for measurement passing it through a hydrogen getter system at liquid nitrogen temperature removing any hydrogen species along with the dominant gas, Ar.   The analysis focused on the two mass numbers 3 and 4 [13].   A summary of the measured amounts of the ^{4}He and ^{3}He is presented in Table.

Table - 1

4 - 1 Standard reactor processed gas sample, ^{4}He less than 0.5 ppm and ^{3}He less than background. (Blank)
4 - 2 Temporal analysis of ^{3}He, run (Ti foil) T transmuting to ^{3}He measured over a 9 month period.
4 - 3 Analysis for ^{3}He and ^{4}He, (Pd foil) ^{4}He at 550 ppm and ^{3}He below background [13].

The gas measurements for generated helium removed from over the D_2O was after 20 hours of cavitation exposure.   The gases were collected from the three reactor runs in sample volumes 4-1, 4-2, 4-3 (Table - 1).   The gases present, besides the helium isotopes and argon were small amounts of D_2O, DOOD, H_2, HD and D_2 which were trapped before measurement [13].   The purity of the Ar gas supplied to us from LANL was checked against a run that produced no helium isotopes.   In the run, 4-1, the ^{4}He found, as determined by Brian Oliver, was less than 0.5ppm in ^{4}He and below background in ^{3}He.   This puts a limit on the amount of ^{4}He in the argon gas cylinder.   This non productive run in helium isotopes can be considered as a blank (^{4}He was measured at (9.9×10^{14} atoms) and ^{3}He was below background).   The sample volume 4-2 which contained the gases from the reactor with the Ti target, produced some ^{4}He (3.1×10^{14} atoms) and ^{3}He that increased with time.   The ^{3}He atoms represent the progressive decay of T atoms residing in the sample volume 4-2.   The sample volume 4-3 produced 1.2×10^{18} atoms of ^{4}He (100 times the concentration found in air) with ^{3}He less than the background measurement of the instrument (a ratio of ^{3}He/^{4}He of less than 10^8)[13].

8. CALORIMETRY

The calorimetric measurements of excess heat generation, $(Q)x$, was based on the performance of the reactor with a Joule heater placed at the $Q(x)$ heat generating point within the reactor.   This allowed for the calibration of the cavitation system. The experimental systems were of two types, the static and the dynamic with regard to D_2O flow.   The dynamic circulation of D2O through the apparatus at its steady-state temperature, involved the heat loss via surface convection losses from a collection of separate components.   These components all differed in their heat loss characteristics because of their geometry, construction materials, and size.   Linked together through the circulation process were the components including a large heat exchanger to remove acoustic, power supply heat, and $Q(x)$.   Thermocouple temperature measurements of the components' surface were logged every minute.   Calibration of the components was accomplished through the use of the monitored Joule heater which replaced the cavitation input during calibration and gave the heat loss characteristics at the steady-state temperatures of the reactor components.   "Newton's Law of Cooling" established a cooling curve for each component (convection cooling) at steady-state temperatures.   The 24 hour

calibration and experimental runs for these individual components, gave us the data where <u>heat out</u> was equal to <u>heat in</u>. During the calibration and cavitation runs, the sum of the heat loss from all components at steady-state was the total <u>heat in</u> from all sources. The Q(x) was determined at steady-state conditions from the calorimetric measured <u>heat out</u> minus the watt meter measured <u>heat in</u>, where the difference must equal zero for calibration runs. The cavitation run measurements when compared to the calibration runs yield a value for Q(x) varying from 0 to 120 watts [10, 23]. The Q(x) of run 4 - 3 was 72 watts which produced 1.2×10^{18} atoms of ^{4}He in 20 hours [13].

9. SUMMARY

The experimental evidence shows that collapsing TCBs produce Q(x), ^{4}He and T. The FE SEM photos of the target foils show the size distribution of the vent size. A possible mechanism for cavitation stimulated fusion in D_2O is proposed that connects the experimental data. A cavitation bubble collapse produces a pinched LEHDP jet of deuterons that is implanted into a target foil. The transient traps of coherent deuterons presents an environment in the lattice for fusion events that leave several kinds of footprints. These are the production of gases of ^{4}He, ^{3}He, and T from the reactor, the SEM of the vent sites (their population size distribution has a maximum population near 24 Mev), and the Q(x) generation. Presented here is a path to sono fusion events that evolved from years of experiments with TCBs. The number of potential implantations and the R_{DD}/J established from the vent population distribution approximates the (Q)x production rates.

ACKNOWLEDGMENTS

REFERENCES

[1] Amasa S. Bishop, *Project Sherwood*; Addison-Wesley (1958)
[2] H. Hora, *Plasmas at High Temperatures and Density*; Roder-Verlag Regensburg, Germany (2000)
[3] L. W. Alvarez, et al, Catalysis of Nuclear Reactions by μ Mesons, *Phys. Rev.*; 105 1127 (1957)
[4] C. Petijean, *Nucl. Phys.*, A543, 79c; (1992)
[5] Yu. V. Petrov, *Nature*; vol 285, 466 ; (1980)
[6] M. Wakatni, *Stellarator and Heliotron Devices*, Oxford University Press, (1998)
[7] *The Jet Project* , Proceedings of a Royal Society Meeting, 12 and 13 March (1986)
[8] L. A. Crum, Sonoluminescence, *Physics Today*; 25 (Sept. 1994)
[9] R. Stringham, R. George, *EPRI Rept.TR-108474*, Mar. (1998).
[10] Roger Stringham, 2001 *Amar. Phys. Sco,*. Seattle WA. MEETING, Mar. 11 - 15 (2001)
[11] R. Stringham, *Proceedings of ICCF-8*, Villa Marigola, LaSpezia, Italy, 299-304 (May 21-26, 2000)
[12] Y.E. Kim, A. L. Zubare,,*ibid,* 375-384 (May 21-26, 2000)
[13] Brian Oliver of DOE performed the helium three analyses measurements. His methodology involved removing all hydrogen species before each analysis (1994 - 5).
[14] R. Stringham; *Proceedings of the IEEE* Ultras. Intern. Symp., Sendai, Japan, vol. 2; 1107 (Oct. 5-8 1998).
[15] L. A. Crum, *J. Phys.*, Paris; 40; 131 (1979)
[16] Y. Tomita, A. Shima; *Acustica*, 71;161, (1990)
[17] M.P. Felix, A. T. Ellis, *Appl. Phys. Lett.* 19, 484 (1971)
[18] W. Lauterborn, H. Bolle, *J Fluid Mech.*,72, 391 (1975)
[19] M. S. Plesset, R. B. Chapman, *J Fluid Mech.* 47, 283 (1971)
[20] J. Kantele, *Nuclear Spectrometry*, Academic Press, (1995).
[21] F. Okuyama, H. Tsujimaki; *Surface Science*; vol. 382, L700-L704 (1997).
[22] H. Yuki, T.Satoh, T. Ohtsuki, T. Yorita, Y. Aoki, H. Yamazaki, J. Kasagi, *Proceedings of ICCF-6,* Japan, 259 (Oct. 13-18,1996).
[23] R. Stringham, 2000 *APS* Minneapolis, MN. Meeting, March 20 - 24 (2000)